

*Supplementary Material*

# Iron Oxide Incorporated Conjugated Polymer Nanoparticles for Simultaneous Use in Magnetic Resonance and Fluorescent Imaging of Brain Tumors

N. Arias-Ramos<sup>1</sup>, L. E. Ibarra<sup>2,4,\*</sup>, M. Serrano-Torres<sup>1</sup>, B. Yagüe<sup>1</sup>, M. D. Caverzán<sup>3,4</sup>, C. A. Chesta<sup>3,5</sup>, R. E. Palacios<sup>3,5</sup> and P. López-Larrubia<sup>1,\*</sup>

**Citation:** N. Arias-Ramos; L.E. Ibarra; M. Serrano-Torres; B. Yagüe; M.D. Caverzán; C.A. Chesta; R.E. Palacios; P. López-Larrubia Iron Oxide Incorporated Conjugated Polymer Nanoparticles for Simultaneous Use in Magnetic Resonance and Fluorescent Imaging of Brain Tumors. *2021*, *13*, 1258. <https://doi.org/10.3390/pharmaceutics13081258>

Academic Editor: Pedro Ramos-Cabrer and Jesus Ruiz-Cabello

Received: 14 July 2021

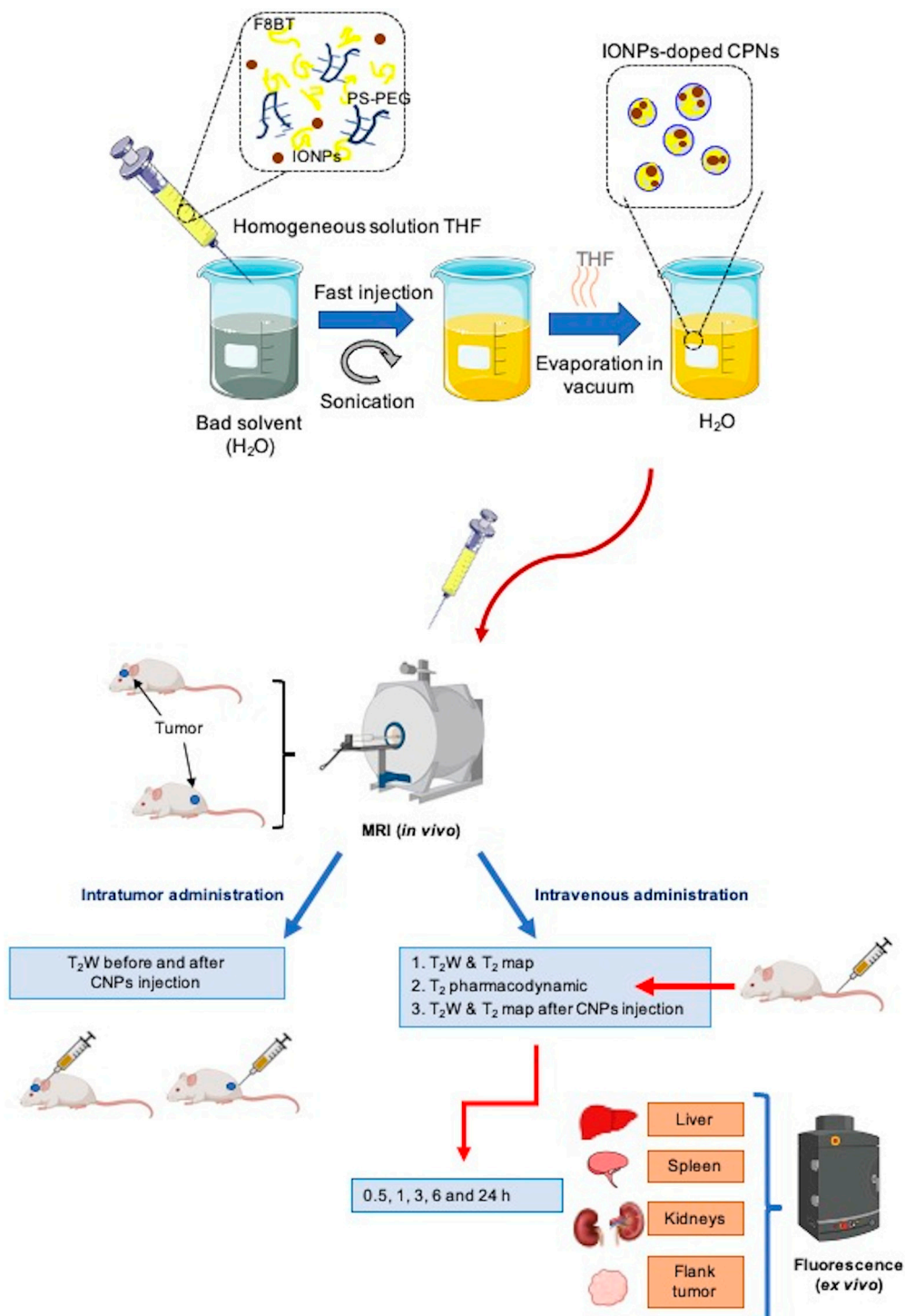
Accepted: 9 August 2021

Published: 14 August 2021

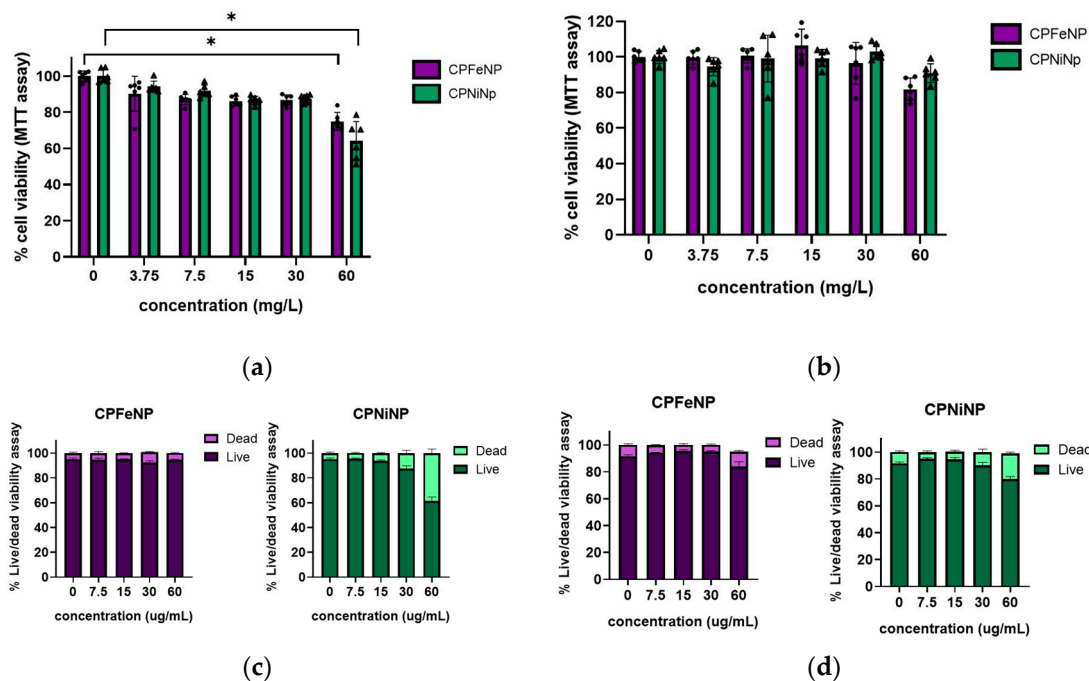
**Publisher's Note:** MDPI stays neutral with regard to jurisdictional claims in published maps and institutional affiliations.



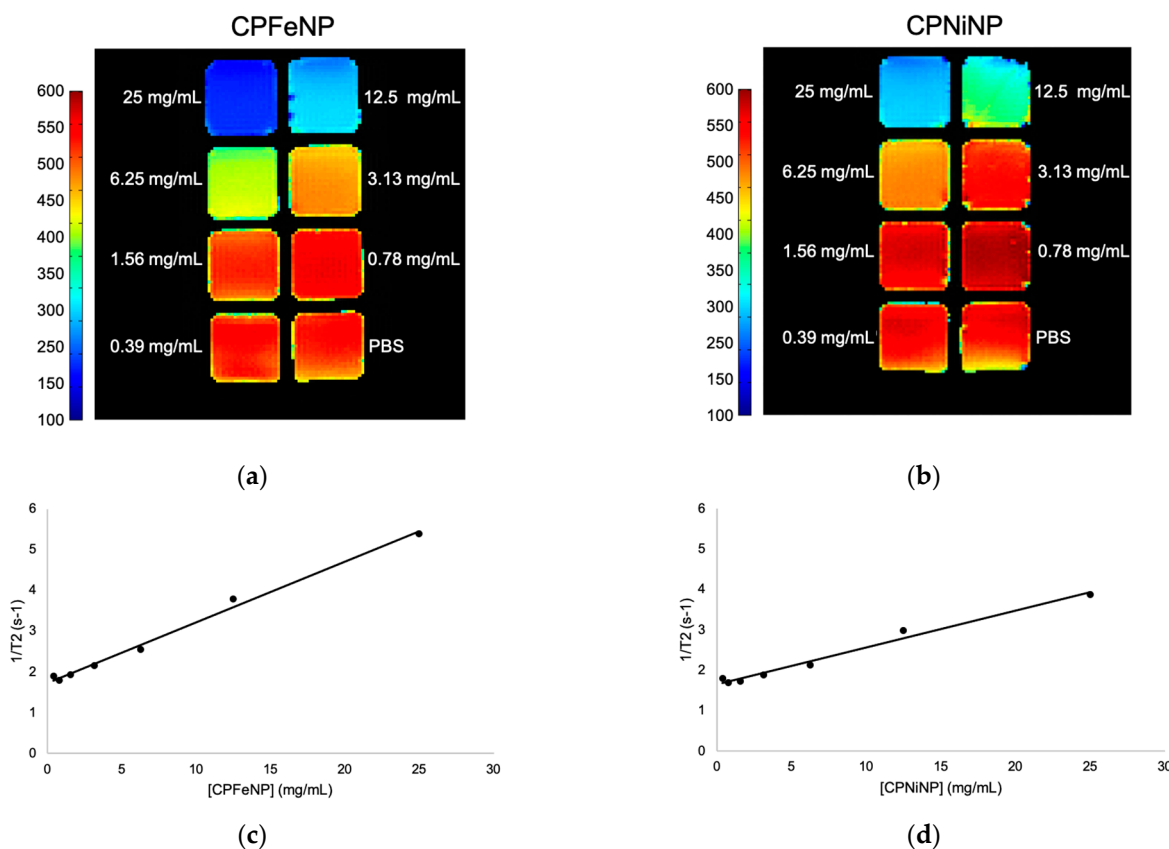
**Copyright:** © 2021 by the authors. Licensee MDPI, Basel, Switzerland. This article is an open access article distributed under the terms and conditions of the Creative Commons Attribution (CC BY) license (<http://creativecommons.org/licenses/by/4.0/>).



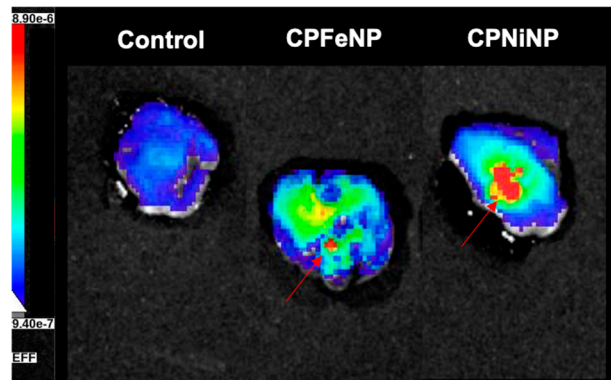
**Figure S1.** Overview of the experimental workflow followed in the preparation, characterization, in vitro and in vivo evaluation of the IONP-doped CPNs. The scheme shows the steps to synthesize and purified the IONP-doped-CNPs in the upper panels and the preclinical assessment of the nanoparticles in the lower.



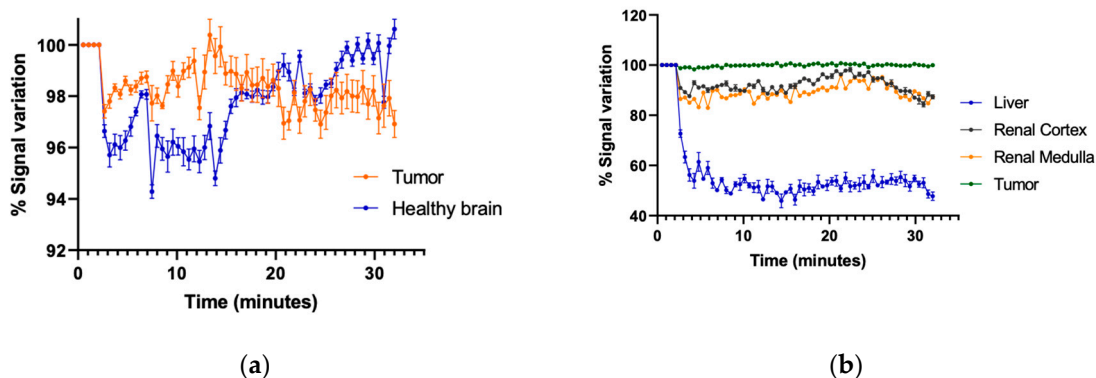
**Figure S2.** Biocompatibility evaluation of IONP-doped CPNs in GBM human cell lines. MTT viability quantification for (a) U-87 MG and (b) T98G. Cell viability quantified by flow cytometry using LIVE/DEAD cell viability assays for (c) U-87 MG and (d) T98G. (\* $p < 0.05$ ).



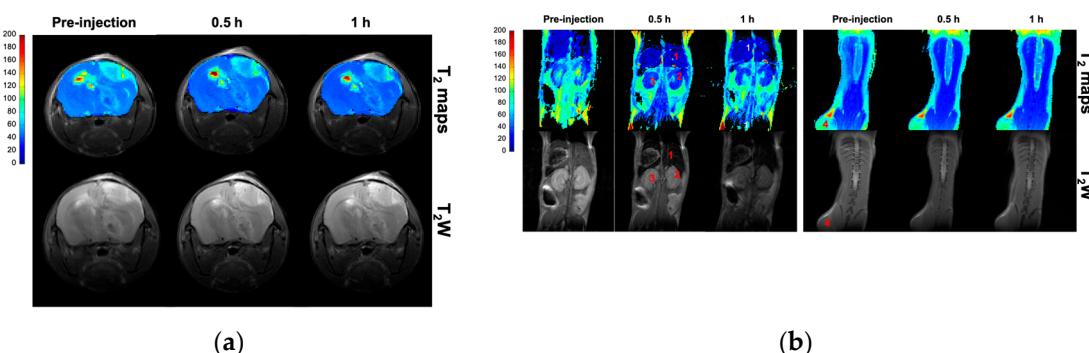
**Figure S3.** Relaxivities determination of IONP-doped CPNs. T<sub>2</sub> maps of nanoparticles at decreasing concentrations: (a) CPFeNP and (b) CPNiNP. Graphical linear regression of relaxation rates (1/T<sub>2</sub>) versus increasing nanoparticle concentration: (c) CPFeNP and (d) CPNiNP.



**Figure S4.** Fluorescence images of tumors after i.t. IONP-doped CPN administration. Images show excised tumors from a control mouse without particle administration (left), a flank tumor after CPFeNP i.t. injection (middle) and a tumor after CPNiNP i.t. injection. Red arrows point to the high fluorescence point due to IONP-doped-CPNs injection.



**Figure S5.** Biodistribution MRI studies of Endorem®. Graphics show the variation in MRI signal intensity (mean  $\pm$  SEM) in the different organs evaluated: tumor and contralateral healthy brain in the orthotopic glioma model (a) and liver, renal cortex, renal medulla and tumor in the heterotopic GBM model (b).



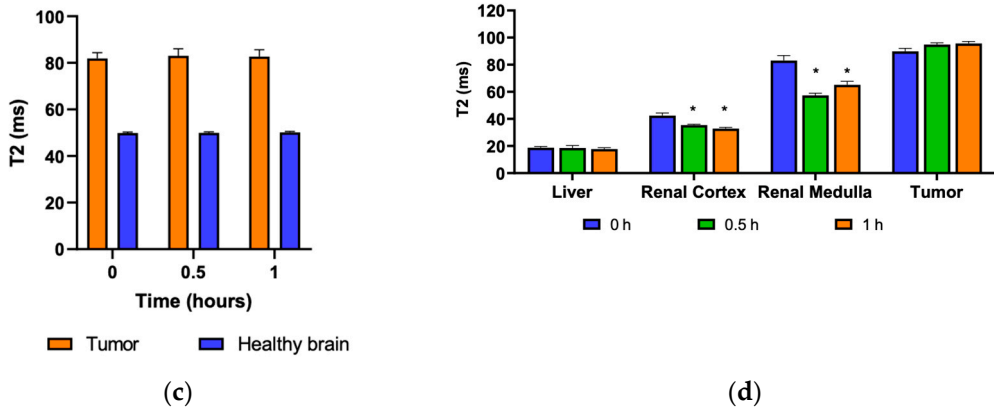


**Figure S6.** T2 maps and T2W images of GBM models injected with Endorem®. T2 color-code based maps and T2W images acquired before the i.v. administration of Endorem®, and at 0.5 and 1 h after the injection, in the of the orthotopic (**a**) and the heterotopic GBM model (**b**), numbers indicate the tissues where the ROIs were selected to do the measurements: 1, liver; 2, renal cortex; 3, renal medulla; 4, flank-tumor. Graphics show the variation in T<sub>2</sub> values (mean ± SEM) of the ROIs along the temporal evaluation in the orthotopic (**c**), and heterotopic tumor bearing mice (**d**). Statistical symbols correspond to the comparison of the data to the pre-injection value. (\* $p < 0.05$ ).